

JLHS: A Joint Linear Frequency Modulation and Hyperbolic Frequency Modulation Approach for Speed Measurement

YUANKUN PENG¹, CAIXIA SONG^{1,2}, LU QI², PENG LIU¹, YIJUN DONG¹,
YAN YANG³, BOYAN ZHANG¹, AND ZHIGUO QI²

¹Hangzhou Institute of Applied Acoustics, Hangzhou 310023, China

²College of Science and Information, Qingdao Agricultural University, Qingdao 266109, China

³School of Electronics and Information, Northwestern Polytechnical University, Xi'an 710072, China

Corresponding author: Caixia Song (cassiesong@qau.edu.cn)

This work was supported in part by the Shandong Smart Ocean Ranch Engineering Technology Collaborative Innovation Center, in part by the Research Fund for High-Level Talents of Qingdao Agricultural University under Grant 1119048, in part by the Shandong Agricultural Science and Technology Service Project under Grant 2019FW037-4, in part by the Horizontal Project under Grant 20193702010792, in part by the Experimental Technical Project of Qingdao Agricultural University under Grant SYJK18-01, and in part by the Ministry of Education Industry-University Cooperation Collaborative Education Project under Grant 201902005027 and Grant 201901029013.

ABSTRACT In the waveform design, the distance measurement and resolution are a pair of irreconcilable contradictions. Linear Frequency Modulation (LFM) can alleviate this contradiction. LFM is widely used in radar and sonar, however, its Doppler tolerance is not ideal. Hyperbolic Frequency Modulation (HFM) signal has a particularly strong tolerance towards Doppler frequency shift. When the unidirectionally modulated HFM signal is in distance measurement, the Doppler delay of the matched filtering output cannot be eliminated, and there is a ranging error. After matched filtering of the positive and negative frequency modulation (HFM+LFM) echo signal based on the same frequency band, the Doppler-induced delay is the same but opposite in direction, and the delay is closely related to the frequency, bandwidth, and pulse width of the transmitted signal. By using the inverse time delay difference of the positive and negative frequency modulation, the ranging error in the ranging of unidirectionally modulated LFM signal can be eliminated. In this paper, a Joint Linear frequency modulation and Hyperbolic frequency modulation approach for Speed measurement (JLHS) is proposed, which employs the same frequency band of positive and negative frequency modulation signals for speed measurement and ranging. Extensive simulation results show that the proposed approach can better estimate the speed and distance of moving targets, and it has reference value for engineering application.

INDEX TERMS Positive and negative frequency modulation, Doppler invariance, speed measurement, distance measurement.

I. INTRODUCTION

Before the occurrence of pulse compression, in the waveform design, the distance measurement and resolution are a pair of irreconcilable contradictions, which can only be compromised. The appearance of pulse compression can solve this problem. Moreover, pulse compression technology has been widely used in radar and sonar [1]–[4]. In a large number of pulse compression signals, the Linear Frequency Modulation (LFM) signal is particularly popular for good

pulse compression performance. LFM contains the following advantages:

- 1) LFM is a Doppler-tolerant waveform, which can tolerate a certain degree of unknown shift in Doppler frequency [5].
- 2) LFM is an equal-amplitude signal, which is beneficial to improve the transmission efficiency of peak power limited systems [6].
- 3) A higher range resolution can be obtained by increasing the bandwidth of LFM.
- 4) In addition, the spectrum of LFM is flat in the frequency band [7], and the generation and processing techniques of LFM are relatively mature [8].

The associate editor coordinating the review of this manuscript and approving it for publication was Jun Shi¹.

According to the above advantages, LFM has been widely used in radar and sonar [9]–[11]. However, a large Doppler frequency shift will cause LFM matched filter mismatch and attenuate the output peak after LFM matched filter [12].

The Hyperbolic Frequency Modulation (HFM) signal is insensitive to Doppler, which can make up for the shortcomings of LFM. The traditional method of speed measurement is, according to the radial velocity of the target relative to the sonar, to calculate the speed through a set of narrow-band filter banks [7]. However, the higher the accuracy of the speed measurement, the more the number of Doppler filter banks needed will be multiplied. Therefore, the cost of the traditional method is too high. In this paper, a Joint Linear frequency modulation and Hyperbolic frequency modulation approach for Speed measurement (JLHS) is proposed, which is based on the same frequency band of positive and negative slope Frequency Modulation (FM) signals. The JLHS method can not only accurately measure the speed, but also greatly decrease the ranging error caused by Doppler frequency shift in unidirectional modulation HFM.

II. RELATED WORK

Song *et al.* [13] modeled the range bias as a function of range rate and system parameters, and then utilized that to calibrate the measurement equation in very precise target tracking. By doing so, the tracking performance can be improved, particularly for fast maneuvering targets. Whyland [14] proposed that Doppler insensitive waveforms, should be used to modulate pulses or sub-pulses of energy for probing a determined environment so that when the modulated energy is transmitted and received, the received energy may be processed. The HFM waveform has an inherent Doppler-invariant property. In order to apply the HFM waveform to existing Inverse Synthetic Aperture Radar (ISAR) imaging systems, Wei *et al.* [15] proposed a new pulse compression algorithm. The pulse compression is accomplished by space-variant phase compensation. In addition, the space-variant phase compensation is realized by resampling and Fast Fourier Transform (FFT) with high computational efficiency. Doisy *et al.* [16] derived the expressions of Doppler tolerance, Doppler and delay accuracy, and delay-Doppler ambiguity in case of high bandwidth duration product signals. The replicas of Doppler estimation and target range were reduced. Finally, results were applied to low-frequency active sonar. Wang *et al.* [17] presented a method by employing the HFM signal as a channel probe to make Doppler estimation and timing synchronization simultaneously. A contrast with the LFM signal adopted in the conventional design was also made. Simulation results showed that the method based on HFM signal had better estimation and more accurate timing synchronization performance. Yang and Sarkar [18] proposed a new polyphase pulse compression codes which were conceptually derived from the step approximation of the phase curve of the hyperbolic frequency modulated chirp signal. The main disadvantage of this polyphase code was the relatively high sidelobe level without Doppler effect, which

can be addressed by applying the proper window function. Yang and Sarkar [19] demonstrated that the acceleration of the target results in a frequency shift which is the source of the signal distortion under the assumption that the acceleration is constant and along the direction of the velocity. Therefore the frequency-shifted version of the matched filter can be applied to eliminate the mismatch between the reflected signal and the matched filter caused by the acceleration of the target. Maric and Titlebaum [20] addressed the problem of constructing frequency hop codes for use in multiuser communication systems such as multiple-access spread-spectrum communications and multiuser radar and sonar systems. The construction of a new family of frequency hopping codes called hyperbolic frequency hop codes was given, and it was shown that the hyperbolic frequency hop codes possessed nearly ideal characteristics for use in both types of system. Zhou *et al.* [21] derived constraints on the HFM parameters to optimally reduce Multiple Access Interference (MAI) at the transmission side. Additional constraints on the frequency-modulation rate reduced the underwater channel effects of multipath and scaling. The proposed signaling scheme was compared to an HFM-based Code-Division Multiple-Access (HFM-CDMA) scheme to demonstrate improved error performance. Lee *et al.* [22] proposed an underwater acoustic communication with hyperbolic frequency modulated waveforms. The received signal was demodulated by matched filtering of received signal and one hyperbolic chirp pulse. Simulation was performed to evaluate the performance of the proposed method. Owing to the large delay spread caused by multipath propagation and the severe Doppler effect of the shallow water acoustic channel, Zhang *et al.* [23] exploited a spread spectrum modulation scheme using HFM signal named as “HFM Spread-Spectrum modulation” (HFM-SS) to substantially improve the performance of communications over such channels. Jiangang *et al.* [24] addressed the problem of Low Probability of Intercept (LPI) techniques. A new LPI signal called PR-FH was brought forward by combining the Barker sequences and hyperbolic frequency hop code and compared with the Phase Shift Keying (PSK) costas-frequency hopping signal. The result showed that the novel waveform has low cross correlation and good resolution of both range and Doppler. Zhou *et al.* [25] developed a fast method for generating HFM radar echoes using static electromagnetic data for HFM waveforms in wideband radar imaging with the computational complexity effectively reduced by phase-matched filtering and frequency domain down-sampling. The result was used to study the influence to HFM signal matched filtering for high-speed movements. This method was also suitable for LFM waveforms. Simulations verified the accuracy and effectiveness of this method. Gini and Giannakis [26] addressed the parameter estimation for a combination of a Polynomial Phase Signal (PPS) and a hyperbolic frequency modulation. Besson *et al.* [27] dealt with parameter estimation of product signals consisting of hyperbolic FM and chirp factors, and presented a computationally simple

algorithm that decouples estimation of the chirp parameters from those of the hyperbolic FM part. Wang *et al.* [28] proposed a method to estimate the target velocity using a combination of two HFM signals. They found that a HFM with an increasing frequency sweep (positive HFM) and one with a decreasing frequency sweep (negative HFM) yield a different time. And a better Doppler estimation can be obtained by using a negative HFM signal followed by a positive HFM signal than the other way around. The method was applied to real data and performance was demonstrated via simulated data. Murray [29] introduced an extended matched filter for HFM waveforms in active sonar systems, along with an exact closed-form solution for the Doppler bias in time of arrival estimates when using this filter. This solution applied to both broadband and narrowband HFM signals. Recently, the hyperbolic-frequency modulated signal has been widely employed in sonar systems for moving targets due to its Doppler tolerance, while the precise velocity estimation becomes a great challenge under such conditions. Huang *et al.* [30] proposed an improved method based on the sliding window matching algorithm to improve the performance. The method controlled the energy of environmental noise and interference by focusing on the dominant target highlight, and applying a designed window which utilizes the Doppler characteristics of hyperbolic-frequency modulated signals. The results verified the influence of the multi-highlights in velocity estimation and indicated that the improved method has more effective performance. Kim *et al.* [31] investigated the performance of HFM signals for timing synchronization in underwater acoustic communication systems. The synchronization performance of the proposed HFM was then evaluated numerically using the channel model constructed based on western sea of South Korea. Numerical analysis suggests the HFM design achieving good performance for timing synchronization in presence of Doppler scale. Jedel *et al.* [32] proposed a sounding signal, which was a combination of Pseudo-Random Sequences (PRS), and elementary signals of HFM type. The structure of this signal was aimed at minimizing measurement error. They presented the idea of a sounding signal of HFM+PRS type, and the results of computer simulations.

Kroszczynski [33] dealt with the problem of wide-band signal optimization for the purpose of minimizing signal degradation resulting from Doppler distortion effects. The equation for the instantaneous frequency of a Doppler-transformed signal was derived. The optimum frequency-modulation law was then shown to be the linear period modulation. Diamant *et al.* [34] presented a method for Doppler-shift estimation based on comparing the arrival times of two chirp signals and approximating the relation between this time difference and the Doppler shift ratio. This analysis also provides an interesting insight about the resilience of chirp signals to Doppler shift. The simulation results demonstrate improvement compared to commonly used benchmark methods in terms of accuracy of the Doppler shift estimation at near-Nyquist baseband sampling rates. LFM signals have

been widely used for target detection in active sonar systems due to their robustness to reverberation. Lee *et al.* [35] proposed a new fast target detection method that was robust to the variation of unknown target speed. The proposed method secured a Signal-to-Noise Ratio (SNR), approaching that of the optimal matched filter output, that was also robust to the variation of target speed and thus it was very useful for the practical use in antitorpedo torpedoes or supercavitating underwater missiles that need to equip low-complexity and robust signal processing systems. Grimmett *et al.* [36] proposed a method that involved using an echo-ranging system to transmit a continuously repeating LFM signal through a propagation medium and receive a return signal reflected off of a target, performing signal processing on the return signal, extracting detected echo sets from the processing intervals, estimating a target range-rate using the estimated time versus delay slopes, computing a bias error using the estimated target range-rate, applying timing correction to the detected echo sets to remove the bias error. Guan *et al.* [37] focused on constructing an optimization model to optimize the LFM-Costas and GSFM pulse trains with the genetic algorithm. The pulse trains can be improved on properties of both ambiguity function and correlations between sub-pulses. The optimized pulse trains were proven to have better detection performance than those of the initial pulse trains. Moreover, it was affirmed that the reverberation suppression performance of pulse trains had also been improved through the optimization model. Huang *et al.* [38] proposed an effective iterative method for parameter estimation of multipath echo. The proposed method retrieves a signal component by searching for the optimal scale factor from the resampling matching outputs, and eliminates the matching output of the estimated signal to analyze the next component. The method prevented the time-domain subtractions of the received signals for providing a higher robustness. Therefore, it can be applied in many fields including active target detection and underwater communication. Boudamouz *et al.* [39] presented Through The Wall (TTW) radar detection simulations with an emerging radar architecture which was the Multiple-Input Multiple-Output (MIMO) radar.

III. THE DESIGN OF POSITIVE AND NEGATIVE FM SIGNAL WAVEFORM

A. HFM TIME DOMAIN WAVEFORM

Let T , f_0 , f_1 and $s(t)$ denote the pulse width of the HFM signal, the starting frequency of the HFM signal, the ending frequency of the HFM signal and the HFM signal changing over time, respectively. Then $s(t)$ can be expressed as follows:

$$s(t) = \begin{cases} e^{-j\varphi_0 \ln(\frac{t'-t}{T})} & 0 \leq t \leq T \\ 0 & \text{otherwise} \end{cases} \quad (1)$$

where $t' = \frac{f_1}{f_1 - f_0} T$ and $\varphi_0 = 2\pi f_0 t'$.

Then $s(t)$ can also be expressed as:

$$s(t) = \begin{cases} e^{-j2\pi f_0 \frac{f_1}{f_1-f_0} T \ln\left(\frac{f_1-f_0}{f_1-f_0} \frac{T-t}{f_1-f_0} \right)} & 0 \leq t \leq T \\ 0 & \text{otherwise} \end{cases} \quad (2)$$

When $f_1 > f_0$, the HFM signal is called positive HFM, denoted as HFM^+ . When $f_0 > f_1$, the HFM signal is called inverse HFM, denoted as HFM^- .

B. LFM TIME DOMAIN WAVEFORM

Let T_l , f_{l0} , f_{l1} and $s_l(t)$ denote the pulse width of the LFM signal, the starting frequency of the LFM signal, the ending frequency of the LFM signal and the LFM signal changing over time, respectively. Then $s_l(t)$ can be expressed as:

$$s_l(t) = \begin{cases} e^{-j2\pi(f_{l0}t + \frac{1}{2}\mu t^2)} & 0 \leq t \leq T_l \\ 0 & \text{otherwise} \end{cases} \quad (3)$$

where μ represents the modulation degree of LFM and $\mu = \frac{B}{T_l}$, and B represents the signal bandwidth of LFM and $B = f_{l1} - f_{l0}$.

When $f_{l1} > f_{l0}$, then the LFM signal is called positive LFM, denoted as LFM^+ . When $f_{l0} > f_{l1}$, then the LFM signal is called negative LFM, denoted as LFM^- .

IV. SPEED MEASUREMENT PRINCIPLE

The higher the frequency used by sonar, the more serious the seawater absorption will be, and the greater the propagation loss will be, which is not conducive to the remote target detection. On the other hand, the electromagnetic waves used by radar to detect submarines in seawater can only travel a few kilometers, and then the energy will be absorbed by the seawater. And thus, in this paper, the formula derivation is based on the baseband low-frequency signal, without any additional carrier frequency, and the bandwidth is within a few hundred Hz, which belongs to Low Power Radio Frequency (LPRF). When the JLHS method is used for radar, just change the parameter values such as bandwidth, frequency band, speed of sound, to radar parameter values.

A. THE EFFECT OF THE SPEED OF THE TARGET ON THE ECHO OF THE HFM SIGNAL

1) THE EFFECT OF THE MOVING SPEED OF THE TARGET ON THE SPECTRUM OF THE HFM^+ SIGNAL

The relative movement between the sonar and the target will cause the received signal to change, which is represented by the shift of the signal frequency, and it is called the Doppler frequency shift phenomenon [40]. Let v represent the speed of the target. It can be seen from Figure 1, when the target moves toward the sonar system, v is positive and the echo frequency increases. Otherwise v is negative and the echo frequency decreases.

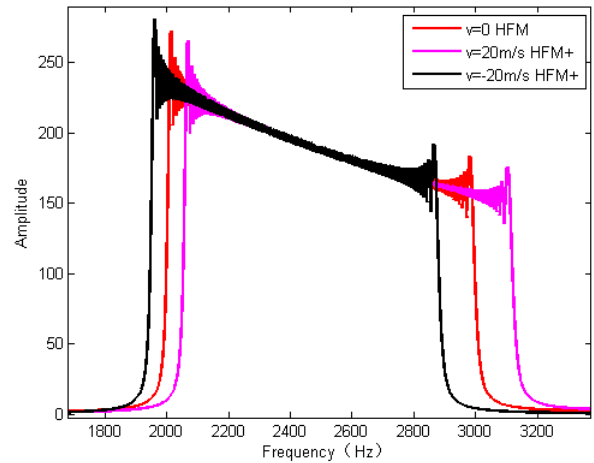


FIGURE 1. Effect of target moving speed on HFM^+ echo spectrum.

2) THE EFFECT OF THE MOVING SPEED AND THE DIRECTION OF THE TARGET ON THE MATCHED FILTERING OF THE FM SIGNAL

The matched processing gain of $10\log(BT)$ can be obtained by employing broadband FM signal and echo matched filtering. It can be seen from Figure 2, with the increase of the moving speed of the target, the main peak value of HFM^+ signal matched filtering output decreases but does not expand [12]. When the direction of the target moving is different, the direction of delay caused by Doppler is also different.

B. THE EFFECT OF THE TARGET SPEED ON THE LFM ECHO SIGNAL

1) THE EFFECT OF THE MOVING SPEED OF THE TARGET ON THE SPECTRUM OF THE LFM^- SIGNAL

Figure 3 shows the effect of the target moving speed on LFM^- echo spectrum. The effect of the moving speed of the target on the spectrum of LFM^- signal is the same as that of the moving speed of the target on the spectrum of HFM^+ signal, which can be seen from Section IV-A-1.

2) THE EFFECT OF THE MOVING SPEED AND THE DIRECTION OF THE TARGET ON THE MATCHED FILTERING OF FM SIGNAL

Figure 4 shows the effect of target speed magnitude and direction on the matching filtering of LFM^- signal. With the increase of the target speed, the main peak value of the matched filtering output of LFM^- signal will not only decrease, but also be broadened [12]. Taking a target moving at uniform speed as an example, the output of LFM after matched filtering is as follows:

$$y = a_1 \left(\tau_1 - \frac{f_d}{\mu} \right) \text{sinc}\left((B - \frac{\omega_d}{2\pi})(t - \tau_2) \right) \times \exp\left[j\left(\frac{\omega_d}{2}(t - \tau_2) + \phi \right) \right] \quad (4)$$

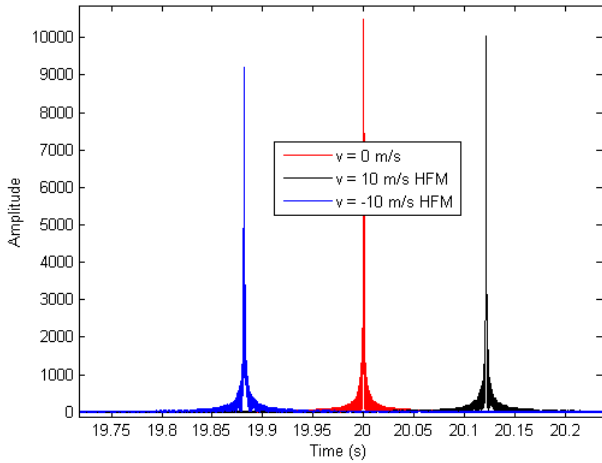


FIGURE 2. Influence of target speed magnitude and direction on HFM+ signal matched filtering.

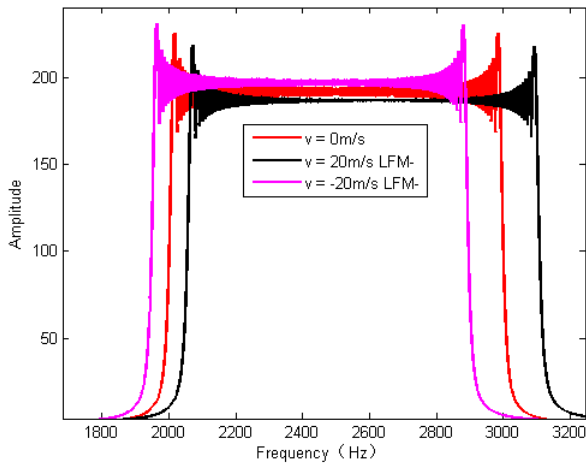
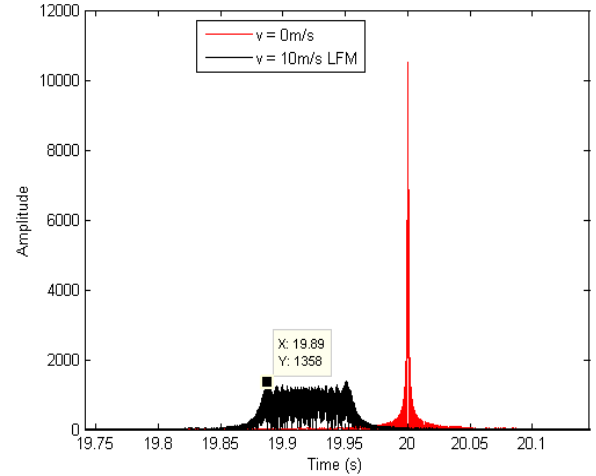


FIGURE 3. Influence of target moving speed on LFM- echo spectrum.

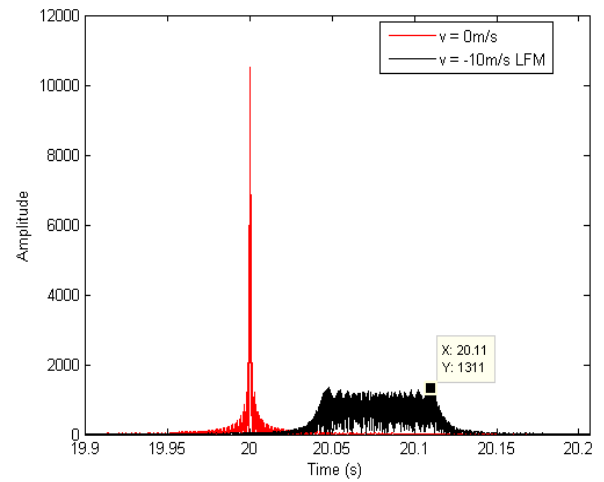
where a_1 , τ_1 , f_d and ω_d represent the ratio of echo to transmitted wave, the delay of the echo arrival time relative to the emission time of the transmitted wave when the target is stationary, Doppler frequency shift and the Doppler frequency shift caused by target movement, respectively. $\phi = \tau_1 \omega_d - \frac{\omega_d^2}{2\mu}$ is a constant and $\tau_2 = t_1 - \frac{f_d}{\mu}$, where t_1 represents the arrival time of echo when the target velocity $v = 0\text{m/s}$.

According to Equation (4), the output of LFM matched filtering is proportional to $t_1 - \frac{f_d}{\mu}$. The frequency used in the simulation sonar is too high, causing the time delay $\frac{f_d}{\mu}$ caused by the target movement to be too large, resulting in the output of the LFM matched filter being too low. The time width and bandwidth product used in simulation is only about 200, and the time width and bandwidth product of the radar are about 10^6 . Therefore, there will be no such obvious difference between high value and low value as shown in Figure 4.

When the movement direction of the target is different, the direction of delay caused by Doppler is also different.



(a)



(b)

FIGURE 4. Effect of target speed magnitude and direction on the matching filtering of LFM- signal.

Note: When the speed is positive, the leftmost time point is selected as the maximum point of the LFM matched filtering output. On the other hand, when the speed is negative, the rightmost time point is selected as the maximum point of the LFM matched filtering output.

C. DOPPLER INVARIANT PRINCIPLE OF HFM

According to the Equation (2), the phase φ of the HFM signal can be calculated by

$$\varphi = 2\pi f_0 \frac{f_1}{f_1 - f_0} T \ln\left(\frac{\frac{f_1}{f_1 - f_0} T - t}{\frac{f_1}{f_1 - f_0} T}\right) \quad (5)$$

Take the derivative with respect to φ , we get its instantaneous frequency $f_s(t)$ is

$$f_s(t) = \frac{d\varphi}{dt} = \frac{f_0 f_1}{f_1 - (f_1 - f_0) \frac{t}{T}} \quad (6)$$

When the target moves at speed v , the relative motion between the sonar and the target causes the transmitted signal with the pulse width T , at the receiving point, to become a signal with a pulse width $\frac{T}{\eta}$. Therefore, the pulse width of the echo is linearly compressed or stretched η times, which can be seen from Figure 5. η can be calculated by

$$\eta = \frac{c + v}{c - v} \quad (7)$$

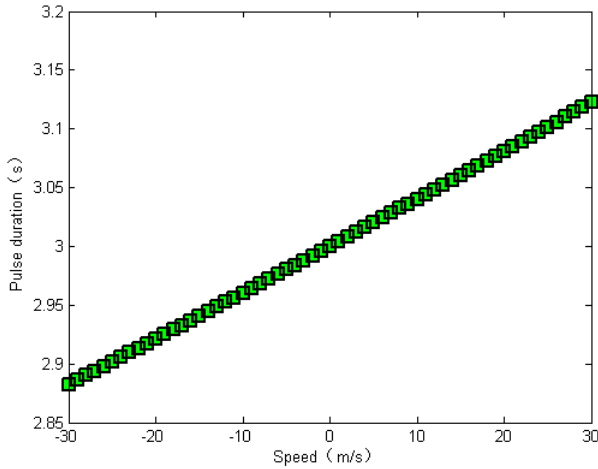


FIGURE 5. Influence of target speed on echo pulse width.

where c represents the speed of sound and its value is equal to 1500 m/s .

According to Equation (5) and Equation (6), the instantaneous frequency $f_r(t)$ of the received echo at this time can be calculated as:

$$f_r(t) = \frac{f_0 f_1}{\frac{f_1}{\eta} - (f_1 - f_0) \frac{t}{T}} \quad (8)$$

Since the HFM signal is insensitive to Doppler, the HFM signal has the characteristic of Doppler invariance. Moreover, the change rule of the instantaneous frequency of the received signal remains unchanged, except that the instantaneous frequency $f_s(t)$ of the original signal is shifted by a time t_0 , as shown in Figure 6, and where t_0 denotes the matched filtering delay due to target Doppler.

Then we let

$$f_r(t) = f_s(t - t_0) \quad (9)$$

According to Equations (6) and (8), t_0 can be obtained.

$$t_0 = \frac{f_1(\frac{1}{\eta} - 1)T}{f_1 - f_0} \quad (10)$$

When the sonar and the target have relative motion, the received signal will produce a frequency shift. Due to HFM signals' Doppler invariance, the instantaneous frequency of the received signal is only a delay. Therefore, a good peak can be obtained by using matched filtering, only the position of the peak has a delay and the amount of the delay is t_0 .

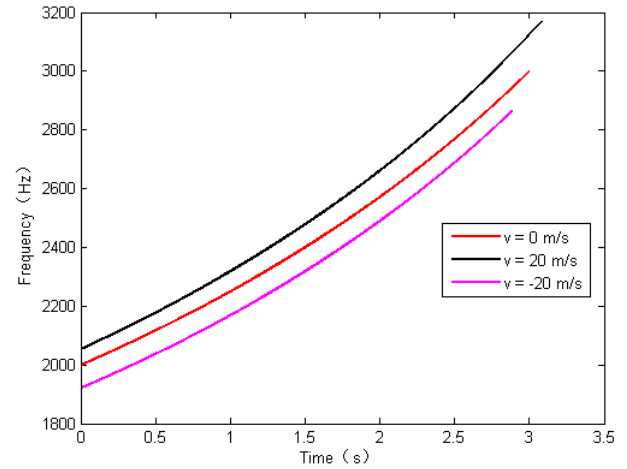


FIGURE 6. The effect of target speed on the HFM⁺ echo spectrum.

However, due to the delay time t_0 caused by Doppler, the distance of the target is determined by the time when the peak of the detector output appears. At this time, the measurement accuracy will be reduced, and there is a ranging error [40].

D. PRINCIPLE OF POSITIVE AND NEGATIVE FM SPEED MEASUREMENT

The processing results of positive and negative slope echo signals through matched filtering are shown in Figure 7. For FM signals with positive and negative slope, the offset size of time delay t_0 of moving targets is the same, and the direction is just opposite [41].

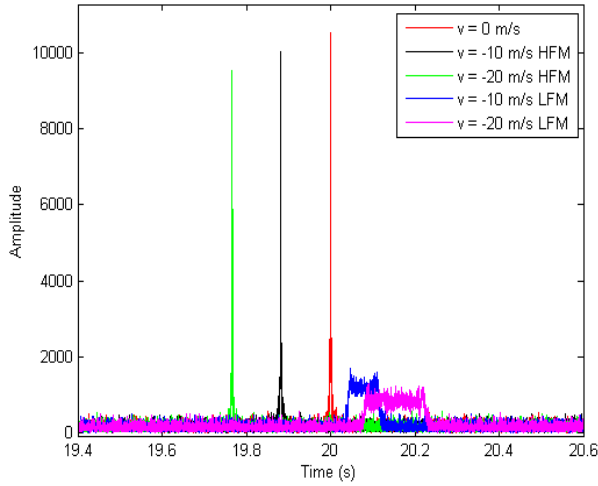
Note: In this paper, the positive and negative slope FM refers to: the frequency of the positive FM signal rising from f_0 to f_1 , and the frequency of the inverse FM signal decreasing from f_1 to f_0 . It can be seen from Figure 8 that, for the positive and negative FM signals, the starting frequency and ending frequency are the same, and the spectrums are the same, but the modulation slopes are different.

V. RANGING AND SPEED MEASUREMENT BASED ON POSITIVE AND NEGATIVE FREQUENCY MODULATION

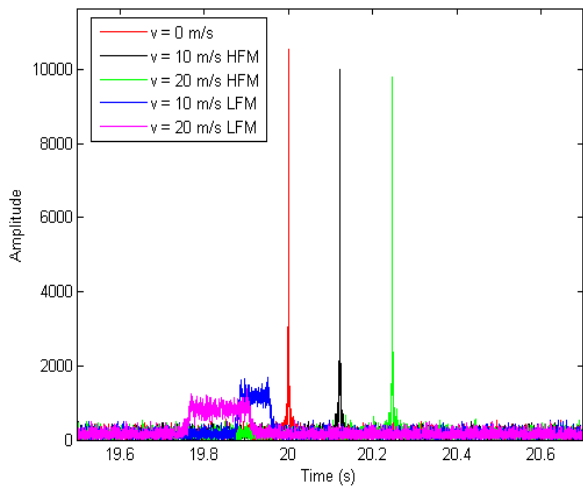
Now let's derive the speed measurement formula. It is assumed that the speed v of the target is positive toward the sonar system, and the positive and negative FM are located in the same frequency band. The signal can be transmitted in either of the following two ways.

- 1) A HFM⁺ signal whose frequency increases with time is first transmitted, and then a LFM⁻ signal whose frequency decreases with time is transmitted.
- 2) A LFM⁺ signal whose frequency increases with time is first transmitted, and then a HFM⁻ signal whose frequency decreases with time is transmitted.

Let t_1 and t_2 represent the time when the matched filtering maximum appears in HFM and LFM, respectively.



(a)



(b)

FIGURE 7. Time delay of the target motion related to the FM signal with the positive and negative slope.

We have

$$t_1 = \frac{2R}{c} + t_0 \quad (11)$$

$$t_2 = \frac{2R}{c} - t_0 \quad (12)$$

where R represents the distance between the sonar transmitting point and the target.

According to Equation (11) and (12), we have

$$\begin{aligned} R &= \frac{(t_1 + t_2) \times c}{4} \\ &= \frac{1}{2} \times c \times \frac{(t_1 + t_2)}{2} \end{aligned} \quad (13)$$

The distance R can also be expressed as:

$$R = \frac{1}{2} \times c \times \tau \quad (14)$$

where τ represents the arrival time of the pulse.

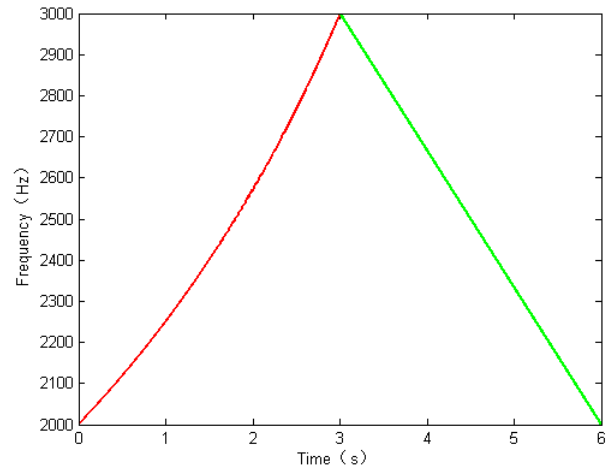


FIGURE 8. Schematic diagram of the spectrum of the positive and negative slope FM signals.

According to Equation (13) and (14), τ is obtained.

$$\tau = \frac{2R}{c} = \frac{(t_1 + t_2)}{2} \quad (15)$$

Based on Equation (15) and Equation (11), t_0 can be calculated as:

$$t_0 = t_1 - \tau \quad (16)$$

According to Equation (7), (10) and (16), the speed v of the target can be calculated as:

$$v = \left(1 - \frac{2}{\frac{1}{\frac{(t_1 - t_2)(f_1 - f_0)}{2} + 1} + 1} \right) \times c \quad (17)$$

Note: The movement direction of the target is judged by the relative magnitude of the maximum value at time t_1 and t_2 at the output of the matched filtering. When the maximum value at time t_1 is greater than the maximum value at time t_2 , the speed direction is negative, and t_1 is the output of HFM and t_2 is the output of LFM. Therefore, time t_2 is the rightmost moment of the maximum value of the output. On the other hand, when the maximum value at time t_1 is less than the maximum value at time t_2 , the speed direction is positive, and t_1 is the output of LFM and t_2 is the output of HFM. Therefore, time t_1 is the leftmost moment of the maximum value of the output.

In Equation (17), the speed v is deduced by HFM, and LFM is only used to find the distance reference point. The speed error v_{err} depends on the SNR and LFM signal, and thus v_{err} can be calculated as:

$$v_{err} = \sqrt{\frac{3}{\frac{2E}{N_0}(\pi T)^2}} \quad (18)$$

where $N_0/2$, E and T represent the noise energy, the signal energy and the pulse width of the signal, respectively.

TABLE 1. Results under simulation environment 1.

SNR	Peak moment		Speed measurement of JLHS (km)	Ranging of JLHS (km)	Speed measurement error of JLHS	Ranging error of JLHS	Ranging error of single signal		Range accuracy improvement ratio	
	t_1	t_2					LFM	HFM	Compared to LFM	Compared to HFM
-20dB	18.76	21.2	14.6658	14.985	2.23%	0.10%	6%	6.20%	98.30%	98.40%
-15dB	18.76	21.19	14.6051	14.9813	2.63%	0.12%	5.93%	6.20%	97.98%	98.10%
-10dB	18.76	21.19	14.6051	14.9813	2.63%	0.12%	5.93%	6.20%	97.98%	98.10%
-5dB	18.76	21.19	14.6051	14.9813	2.63%	0.12%	5.93%	6.20%	97.98%	98.10%

TABLE 2. Results under simulation environment 2.

Speed	Peak moment		Speed measurement of JLHS (km)	Ranging of JLHS (km)	Speed measurement error of JLHS	Ranging error of JLHS	Ranging error of single signal		Range accuracy improvement ratio	
	t_1	t_2					LFM	HFM	Compared to LFM	Compared to HFM
20m/s	18.34	21.73	20.4537	15.0262	2.27%	0.17%	8.30%	8.65%	97.95%	98.03%
-15m/s	18.76	21.19	14.6658	14.985	2.23%	0.10%	6%	6.20%	98.33%	98.39%
5	19.58	20.42	4.9834	15	1.99%	0%	2.10%	2.10%	100%	100%
3	19.76	20.26	2.9821	15.0075	0.60%	0.01%	1.20%	1.30%	99.58%	99.62%

The LFM signal and HFM signal in the combined signals occupy the same frequency band and have the same pulse width, so the energy of the two signals is the same. After the combined signals pass through the matched filter, at the output of the filter, the maximum value of the output signals is equal to the energy E of the signals. Under the condition of low frequency fundamental frequency, the transmitted combined signal waveform is reflected by the moving target to form an echo signal. After the echo passes through the matching filter, the output peak attenuation of LFM is relatively large, and there is a serious broadening phenomenon of the main peak, leading to the energy dispersion. On the other hand, for HFM, because of its Doppler non-deformation, its peak attenuation is small, and there is no broadening of the main peak, and its energy is relatively concentrated. Due to the difference between LFM and HFM, the combined signals of HFM and LFM will produce two peaks, one high and one low, after passing through the matched filter. Therefore, the height of the two peaks can be used to determine the direction of the target speed.

In low SNR or clutter environments, the effect of noise on the two signals in the combination signal of the same frequency band and the same pulse width is the same, unless the SNR is so weak that the LFM echo cannot have a peak. Otherwise, as long as two peaks can appear, there will be one high and one low. The peak is the output after HFM matched filtering, and the low peak is the output after LFM matched filtering.

The JLHS is a speed measurement method, and it is based on the principle that, after the positive and negative FM combined signal matched filtering, the moving target has opposite delay direction. Therefore, the JLHS method is also suitable for radar and multi-radar scenarios.

VI. PERFORMANCE ANALYSIS

A. SIMULATION SETTINGS

We set up two simulation environments for experimental comparison: Simulation Environment 1 and Simulation Environment 2.

Simulation Environment 1: The pulse width of LFM signal $T = 3s$ and sampling frequency $f_{sa} = 7000Hz$. The speed of the target is $-15m/s$. The distance between target and sound source is 15km. In the echo signal, the

SNR is $-20dB$. The starting and ending frequency of positive and negative FM are $f_0 = 2000Hz$ and $f_1 = 2100Hz$, respectively.

Simulation Environment 2: The pulse width of LFM signal $T = 3s$ and sampling frequency $f_{sa} = 7000Hz$. The speed of the target is $20m/s$. The distance between target and sound source is 15km. In the echo signal, the SNR is $-20dB$. The starting and ending frequency of positive and negative FM are $f_0 = 2000Hz$, $f_1 = 2100Hz$, respectively.

B. SIMULATION RESULTS

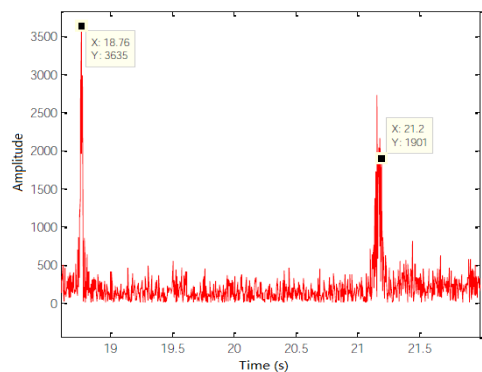
Figure 9 shows the performance analysis under the simulation environment 1 under various SNRs, and Table 1 gives the numerical results of JLHS, LFM and HFM.

We take Figure 9(a) as an example to analyze the performance of JLHS method under various SNRs. From Figure 9(a), it can be seen that, in the JLHS method, after matched filtering, the maximum points $t_1 = 18.76$ and $t_2 = 21.2$. Based on Equation (13), R is equal to 14.9850km. According to Equation (17), the value of v is 14.6658m/s. The ranging error and the speed measurement error of JLHS are 0.1% and 2.23%, respectively. The ranging error of LFM and HFM are 6% and 6.2%, respectively. It can be seen from Table 1 that, compared with LFM and HFM, the range measurement accuracy of JLHS is improved by 98.3% and 98.4%, respectively.

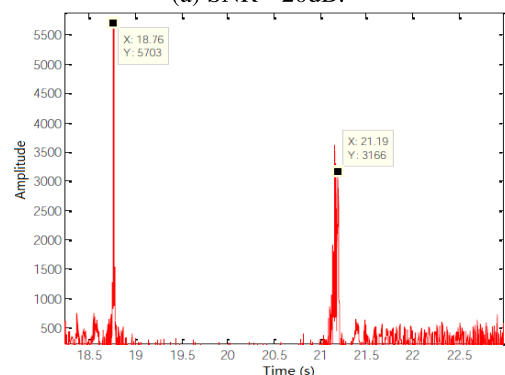
Figure 10 shows the performance analysis under the simulation environment 2 under various v , and Table 2 gives the numerical results of JLHS, LFM and HFM.

We take Figure 10(a) as an example to analyze the performance of JLHS method under various v . From Figure 10(a), it can be seen that, in the JLHS method, after matched filtering, the maximum points $t_1 = 18.34$ and $t_2 = 21.73$. Based on Equation (13), R is equal to 15.0262km. According to Equation (17), the value of v is 20.4537m/s. The ranging error and the speed measurement error of JLHS are 0.17% and 2.27%, respectively. The ranging error of LFM and HFM are 8.3% and 8.65%, respectively. It can be seen from Table 2 that, compared with LFM and HFM, the range measurement accuracy of JLHS is improved by 97.95181% and 98.03468%, respectively.

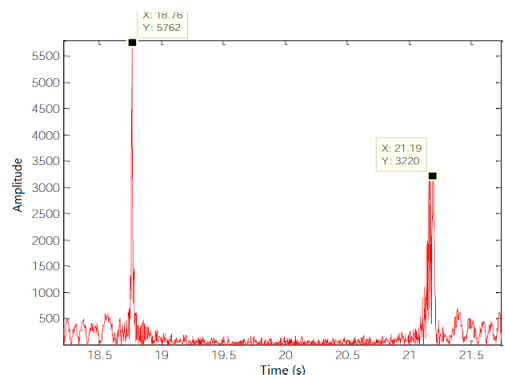
The smaller the target moving speed, the smaller the Doppler frequency shift f_d , which makes the mismatch



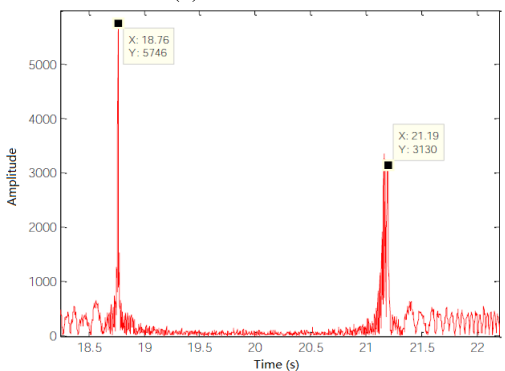
(a) SNR=-20dB.



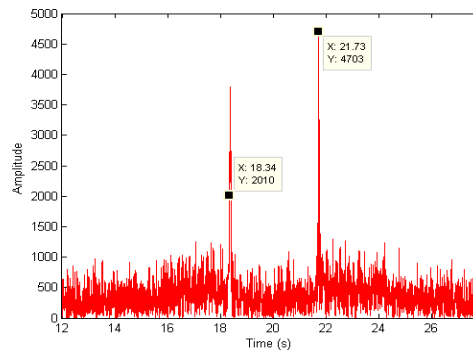
(b) SNR=-15dB.



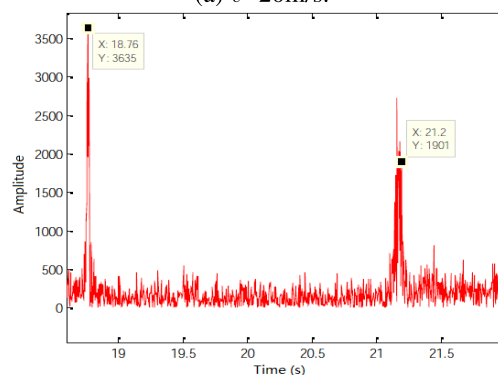
(c) SNR=-10dB.



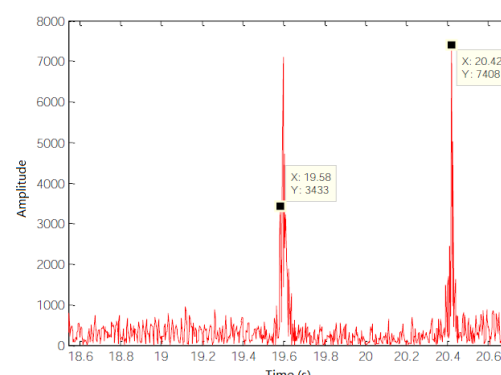
(d) SNR=-5dB.



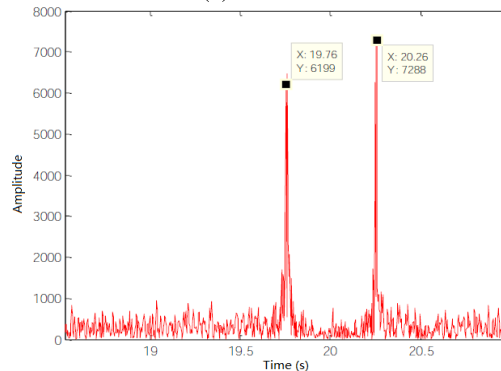
(a) $v=20\text{m/s}$.



(b) $v=15\text{m/s}$.



(c) $v=5\text{m/s}$.



(d) $v=3\text{m/s}$.

FIGURE 9. The output of matched filtering under various SNRs.

FIGURE 10. The output of matched filtering under various the speed of the target.

caused by LFM matched filtering smaller and the amplitude reduction after LFM pulse compression smaller. Therefore, in a low Doppler environment, detection is easier and more accurate. On the other hand, when positive and negative HFM is measuring the speed, it can also eliminate the ranging error caused by Doppler delay t_0 in single HFM signal. Therefore, due to employing the positive and negative HFM, JLHS method can not only measure the speed, it can also improve the ranging accuracy.

VII. CONCLUSION AND FUTURE WORKS

The traditional single HFM or LFM signal can only measure the distance, but can not measure the velocity. When measuring the distance, the single signal is easily affected by the time delay t_0 caused by Doppler, and then there are ranging errors. In this paper, a Joint Linear frequency modulation and Hyperbolic frequency modulation approach for Speed measurement (JLHS) is proposed. The JLHS method can not only measure the velocity accurately, but also eliminate the ranging errors of the time delay t_0 caused by Doppler in single traditional signals.

To improve the accuracy of the positive and negative FM speed measurement, that is, at the same speed, the matched filtering delay t_0 caused by the Doppler of the target is as large as possible. According to Equation (10), there are three ways to improve t_0 : 1) Increase the frequency f_1 ; 2) Decrease the bandwidth ($f_1 - f_0$); 3) Increase the pulse width T . Each way requires additional hardware costs, and the complexity of the entire system must be considered comprehensively.

The basis of JLHS method for speed measurement and ranging is that LFM and HFM signals can be detected, and the peak value after matched filtering is higher than background noise. In the future, we will study the ranging and speed measurement method under too low SNR or clutter environments.

REFERENCES

- [1] E. De Witte and H. D. Griffiths, "Improved ultra-low range sidelobe pulse compression waveform design," *Electron. Lett.*, vol. 40, no. 22, pp. 1448–1450, Oct. 2004.
- [2] M. V. N. Rao and K. R. Rajeswari, "Target detection with cross ambiguity function using binary sequences with high discrimination," *Int. J. Comput. Appl.*, vol. 16, no. 4, pp. 8–12, Feb. 2011.
- [3] M.-A. Govoni, *Linear Frequency Modulation of Stochastic Radar Waveform*. Hoboken, NJ, USA: Stevens Institute of Technology, 2011.
- [4] K. Huo, B. Deng, Y. Liu, W. Jiang, and J. Mao, "High resolution range profile analysis based on multicarrier phase-coded waveforms of OFDM radar," *J. Syst. Eng. Electron.*, vol. 22, no. 3, pp. 421–427, Jun. 2011.
- [5] M. I. Skolnik, *Introduction to Radar Systems*. New York, NY, USA: McGraw-Hill, 1990.
- [6] L. Patton, S. Frost, and B. Rigling, "Efficient design of radar waveforms for optimised detection in coloured noise," *IET Radar, Sonar Navigat.*, vol. 6, no. 1, pp. 21–29, 2012.
- [7] Q. Li, *Digital Sonar Design in Underwater Acoustics: Principles and Applications*. Anhui Education Press, 2003.
- [8] M. Luszczek and A. Labudzinski, "Sidelobe level reduction for complex radar signals with small base," in *Proc. 13th Int. Radar Symp.*, May 2012, pp. 146–149.
- [9] X. Ai, Y. Li, X. Wang, and S. Xiao, "Some results on characteristics of bistatic high-range resolution profiles for target classification," *IET Radar, Sonar Navigat.*, vol. 6, no. 5, pp. 379–388, Jun. 2012.
- [10] P. R. White and J. Locke, "Performance of methods based on the fractional Fourier transform for the detection of linear frequency modulated signals," *Signal Process., IET*, vol. 6, no. 5, pp. 478–483, Jul. 2012.
- [11] O. Klinger, Y. Stern, T. Schneider, K. Jamshidi, and A. Zadok, "Long microwave-photonics variable delay of linear frequency modulated waveforms," *IEEE Photon. Technol. Lett.*, vol. 24, no. 3, pp. 200–202, Feb. 1, 2012.
- [12] P. Yuhong, Y. Qi, and W. Shichuang, "Research on hyperbolic frequency modulation signal speed and ranging method," *Acoust. Electr. Eng.*, no. 4, pp. 21–24, 2014.
- [13] X. Song, P. Willett, and S. Zhou, "Range bias modeling for Hyperbolic-Frequency-Modulated waveforms in target tracking," *IEEE J. Ocean. Eng.*, vol. 37, no. 4, pp. 670–679, Oct. 2012.
- [14] W. P. Whyland, "Doppler consistent hyperbolic frequency modulation," U.S. Patent 5077 702, Dec. 31, 1991.
- [15] Z. Wei, Y. Chunmao, J. Kan, L. Yaobin, and Y. Jian, "Radar echo generation for hyperbolic frequency-modulation waveforms," *J. Tsinghua Univ. (Sci. Technol.)*, vol. 55, no. 8, pp. 878–883, 2015.
- [16] Y. Doisy, L. Deruaz, S. P. Beerens, and R. Been, "Target Doppler estimation using wideband frequency modulated signals," *IEEE Trans. Signal Process.*, vol. 48, no. 5, pp. 1213–1224, May 2000.
- [17] K. Wang, S. Chen, C. Liu, Y. Liu, and Y. Xu, "Doppler estimation and timing synchronization of underwater acoustic communication based on hyperbolic frequency modulation signal," in *Proc. IEEE 12th Int. Conf. Neww., Sens. Control*, Apr. 2015, pp. 75–80.
- [18] J. Yang and T. K. Sarkar, "A new Doppler-tolerant polyphase pulse compression codes based on hyperbolic frequency modulation," in *Proc. IEEE Radar Conf.*, Apr. 2007, pp. 265–270.
- [19] J. Yang and T. K. Sarkar, "Acceleration-invariant pulse compression using hyperbolic frequency modulated waveforms," in *Proc. Int. Waveform Diversity Design Conf.*, Jan. 2006, pp. 1–5.
- [20] S. V. Maric and E. L. Titlebaum, "A class of frequency hop codes with nearly ideal characteristics for use in multiple-access spread-spectrum communications and radar and sonar systems," *IEEE Trans. Commun.*, vol. 40, no. 9, pp. 1442–1447, Sep. 1992.
- [21] M. Zhou, J. J. Zhang, and A. Papandreou-Suppappola, "Hyperbolic frequency modulation for multiple users in underwater acoustic communications," in *Proc. IEEE Int. Conf. Acoust., Speech Signal Process. (ICASSP)*, May 2014, pp. 3498–3502.
- [22] C.-E. Lee, H.-W. Lee, K.-M. Kim, W.-S. Kim, S.-Y. Chun, and S.-K. Lee, "Underwater communication with amplitude-hyperbolic frequency modulation," in *Proc. 6th Int. Conf. Ubiquitous Future Netw. (ICUFN)*, Jul. 2014, pp. 560–561.
- [23] L. Zhang, X. Xu, W. Feng, and Y. Chen, "HFM spread spectrum modulation scheme in shallow water acoustic channels," in *Proc. Oceans*, Oct. 2012, pp. 1–6.
- [24] H. Jingang, T. Ran, S. Tao, and Q. Lin, "A novel LPI radar signal based on hyperbolic frequency hopping combined with barker phase code," in *Proc. 7th Int. Conf. Signal Process.*, vol. 3, Aug./Sep. 2004, pp. 2070–2073.
- [25] W. Zhou, C.-M. Yeh, K. Jin, J. Yang, and Y.-B. Lu, "ISAR imaging based on the wideband hyperbolic frequency-ModulationWaveform," *Sensors*, vol. 15, no. 9, pp. 23188–23204, Sep. 2015.
- [26] F. Gini and G. B. Giannakis, "Parameter estimation of hybrid hyperbolic FM and polynomial phase signals using the multi-lag high-order ambiguity function," in *Proc. Conf. Rec. 31st Asilomar Conf. Signals, Syst. Comput.*, vol. 1, Nov. 1997, pp. 250–254.
- [27] O. Besson, G. B. Giannakis, and F. Gini, "Improved estimation of hyperbolic frequency modulated chirp signals," *IEEE Trans. Signal Process.*, vol. 47, no. 5, pp. 1384–1388, May 1999.
- [28] F. Wang, S. Du, W. Sun, Q. Huang, and J. Su, "A method of velocity estimation using composite hyperbolic frequency-modulated signals in active sonar," *J. Acoust. Soc. Amer.*, vol. 141, no. 5, pp. 3117–3122, May 2017.
- [29] J. J. Murray, "On the Doppler bias of hyperbolic frequency modulation matched filter time of arrival estimates," *IEEE J. Ocean. Eng.*, vol. 44, no. 2, pp. 446–450, Apr. 2019.
- [30] S. Huang, S. Fang, and N. Han, "An improved velocity estimation method for wideband multi-highlight target echoes in active sonar systems," *Sensors*, vol. 18, no. 9, p. 2794, Aug. 2018.
- [31] M.-S. Kim, T.-H. Im, Y.-H. Cho, K.-W. Kim, and H.-L. Ko, "HFM design for timing synchronization in underwater communications systems," in *Proc. OCEANS-Aberdeen*, Jun. 2017, pp. 1–4.
- [32] A. Jedel, J. Marszal, and R. Salamon, "Continuous wave sonar with hyperbolic frequency modulation keyed by pseudo-random sequence," *Hydroacoustics*, vol. 19, pp. 185–196, 2016.

- [33] J. J. Kroszczynski, "Pulse compression by means of linear-period modulation," *Proc. IEEE*, vol. 57, no. 7, pp. 1260–1266, Jul. 1969.
- [34] R. Diamant, A. Feuer, and L. Lampe, "Choosing the right signal: Doppler shift estimation for underwater acoustic signals," in *Proc. 7th ACM Int. Conf. Underwater Netw. Syst. (WUWNet)*, New York, NY, USA, 2012, p. 27, doi: 10.1145/2398936.2398971.
- [35] D.-H. Lee, J.-W. Shin, D.-W. Do, S.-M. Choi, and H.-N. Kim, "Robust LFM target detection in wideband sonar systems," *IEEE Trans. Aerosp. Electron. Syst.*, vol. 53, no. 5, pp. 2399–2412, Oct. 2017.
- [36] D. J. Grimmitt, "System and method for target Doppler estimation and range bias compensation using high duty cycle linear frequency modulated signals," U.S. Patent 9 465 108, Oct. 11, 2016.
- [37] C. Guan, Z. Zhou, and X. Zeng, "Optimal waveform design using frequency-modulated pulse trains for active sonar," *Sensors*, vol. 19, no. 19, p. 4262, Sep. 2019.
- [38] S. Huang, S. Fang, and N. Han, "Iterative matching-based parameter estimation for time-scale underwater acoustic multipath echo," *Appl. Acoust.*, vol. 159, Feb. 2020, Art. no. 107094.
- [39] B. Boudamouz, P. Millot, and C. Pichot, "Through the wall MIMO radar detection with stepped frequency waveforms," in *Proc. 7th Eur. Radar Conf.*, Sep./Oct. 2010, pp. 400–402.
- [40] T. Tan, *Sonar Technology*. Harbin, China: Harbin Engineering Univ. Press, 2010.
- [41] R. Guo, Z. M. Cai, and Z. X. Yao, "Sidelobe suppression method of linear frequency modulated pulse compression signal," *J. Jiangsu Univ. Sci. Technol. (Natural Sci. Ed.)*, vol. 36, no. 2, pp. 298–303, 2014.



PENG LIU was born in Qingdao, China, in 1980. He received the M.S. degree. His research interests include sonar overall design technology, underwater acoustic signal processing, and so on.



YIJUN DONG was born in 1973. He is currently a Researcher. His main research interest includes signal processing



YUANKUN PENG received the B.S. degree in electronic information engineering from Qingdao Agricultural University, Qingdao, China, in 2013, and the M.S. degree in signal processing from Northwestern Polytechnical University, Xi'an, China, in 2016. His research interest includes signal processing.



YAN YANG received the Ph.D. degree. She is currently a Professor with the School of Electronic Information, Northwestern Polytechnical University. She undertakes a number of national, provincial, and municipal planning projects. Her research interests include signal detection and estimation and multi-sensor information fusion.



CAIXIA SONG received the B.S. degree in computer science and technology from the Shijiazhuang Army Command College, Shijiazhuang, China, in 2000, the M.S. degree in computer science and technology from Shandong University, Jinan, China, in 2004, and the Ph.D. degree in computer science and technology from the Dalian University of Technology, Dalian, China, in 2018. Her research interests include vehicular ad hoc wireless network communication, resource management, congestion control, application of machine learning, and block chain technology in intelligent agriculture.



BOYAN ZHANG was born in 1990. He received the B.S. degree from Harbin Engineering University, China, in 2012. His main research interest includes signal processing.



LU QI was born in 1999. He is currently pursuing the bachelor's degree in electronic information engineering with Qingdao Agricultural University. His main research interests include signal processing, blockchain technology, and privacy protection.



ZHIGUO QI is currently pursuing the bachelor's degree with Qingdao Agricultural University. His main research interests include distributed node communication and distributed computing.

...